Electronic Supplementary Material (ESI) for ChemComm.

Supporting Information for

Anion binding modes in *cis/trans*–isomers of binding site–fluorophore–*π*-extended system

Min Zhou,[†] Jinju Chen,[†] Chuanxiang Liu,[*,†] Hanghai Fu,[†] Nan Zheng,[‡] Chuanxiu Zhang,[†] Yong Chen[†] and Jiagao Cheng[‡]

[†]School of Chemical and Environmental Engineering, Shanghai Institute of Technology, Shanghai 201418, China

[‡]Shanghai Key Laboratory of Chemical Biology, School of Pharmacy, East China University of Science and Technology, Shanghai 200237, China

e-mail: cxliu@sit.edu.cn;

Contents of Supporting Information

1. General methods.

Unless otherwise noted, solvents and reagents were analytical grade and used without further purification. THF were distilled from Na prior to use. Flash chromatography was carried out on silica gel (200–300 mesh). UV-vis absorption spectra were obtained on a SHIMADZU UV-1800 spectrophotometer. Fluorescence emission spectra were obtained on a Hitach F-4600 Fluorescence spectrophotometer. IR were recorded on NICOLET 6700 FT-IR. ^{1}H NMR and ^{13}C NMR spectra were recorded on Bruker AVANCE III 500 MHz and 400 MHz (operating at 500 MHz for ^{1}H NMR and 100 MHz for ^{13}C NMR), and chemical shifts were reported in parts per million (ppm, δ) downfield from internal standard Me_4Si (TMS). HRMS were recorded on solan X 70 FT-MS spectrometer with methanol and water (v/v = 1:1) as solvent. Melting points were determined using melting point apparatus (WRS-2A) and uncorrected. Multiplicities of signals are described as follows: s --- singlet, br. s --- broad singlet, d --- doublet, t --- triplet, m --- multiplet.

2. Synthesis routes of dosimeter 3 (*cis*, *trans*) and its ketone derivatives 4 (*cis*, *trans*).

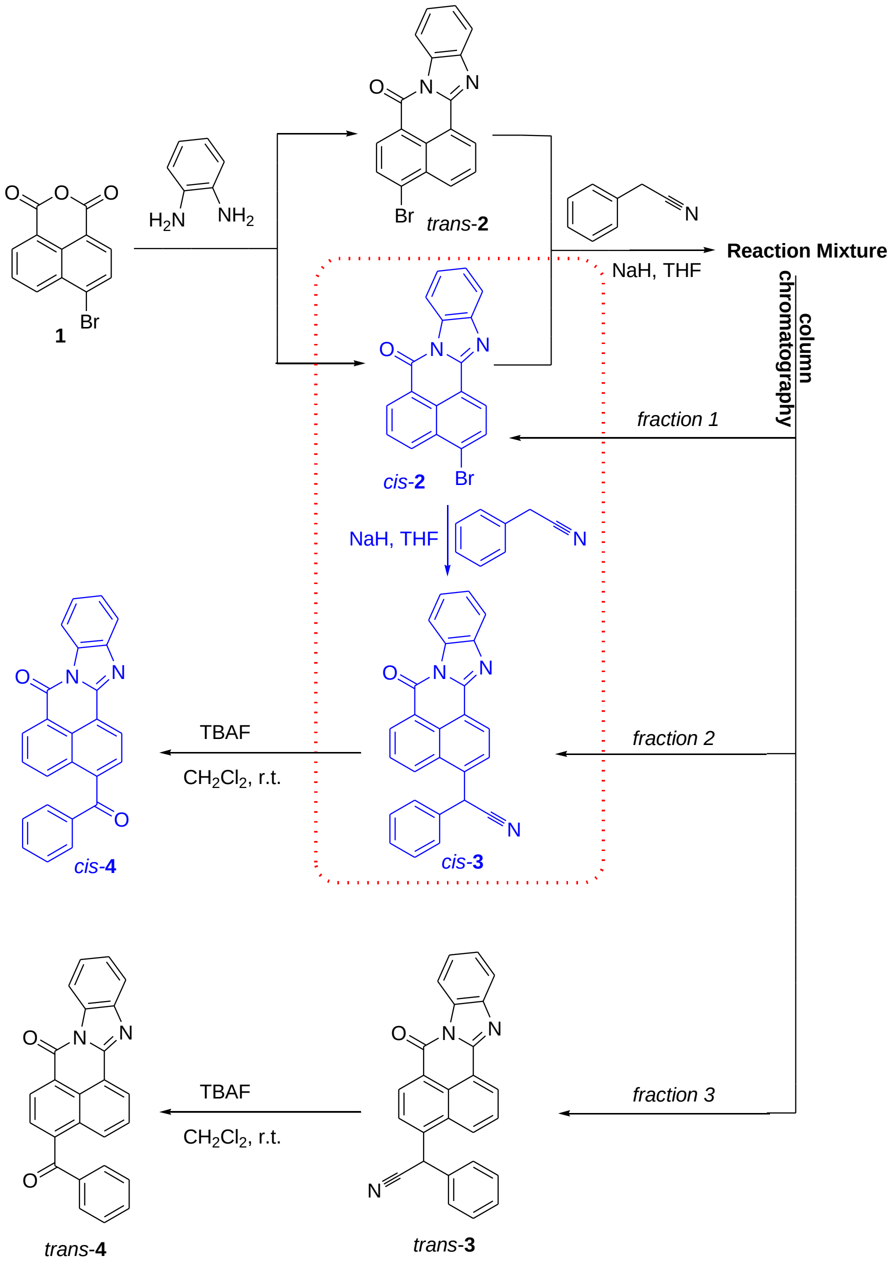

Description: The compounds *cis*-**3** and *trans*-**3** were synthesized using the following methods[1-6]: 4-bromo-1,8-naphthalenedicarboxylic anhydride (**1**) reacted with *o*-phenylenediamine to give the isomers *cis*-**2** and *trans*-**2**, which was further condensed with phenylacetonitrile to afford the mixture of c*is*-**3** and *trans*-**3**. The mixture of isomers was purified by column chromatography on silica gel, affording pure unreactive starting material *cis*-**2**, target compounds *cis*-**3** and *trans*-**3**. The separated component, *cis*-**2**, was further transformed to isomer *cis*-**3** by the similar workup. Moreover, the oxidative decyanation of isomers c*is*-**3** and *trans*-**3** with TBAF afforded the corresponding isomers c*is*-**4** and *trans*-**4**, respectively.

3. Synthesis and characterization of 2–4 (*cis*, *trans*).

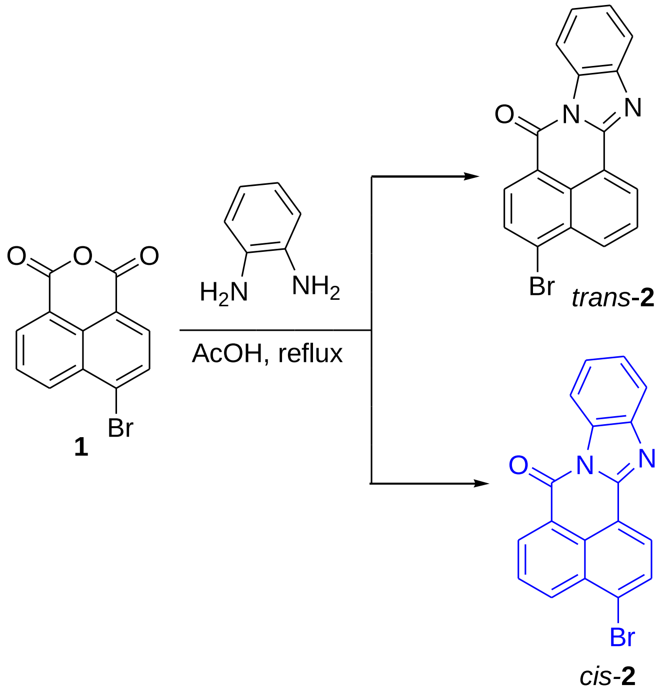

Synthesis of bromo-7*H*-benz[*de*]benzimidazo[2,1-*a*]isoquinoline-7-ones (*trans*-2 and *cis*-2): To an acetic acid solution (25 mL) of 4-bromo-1,8-naphthalenedicarboxylic anhydride (**1**, 2.76 g, 10 mmol) was added *o*-phenylenediamine (1.10 g, 10 mmol), and the mixture was refluxed for 3 h. After the reaction was completed by TLC analysis, the mixture was poured into ice water (50 mL). The resulting precipitate was filtered and purified by recrystallization from toluene. The residues were dried 6 h at 80 °C to afford the pure mixtures of *cis*-**2** and *trans*-**2** (3.00 g, 85.6 %).

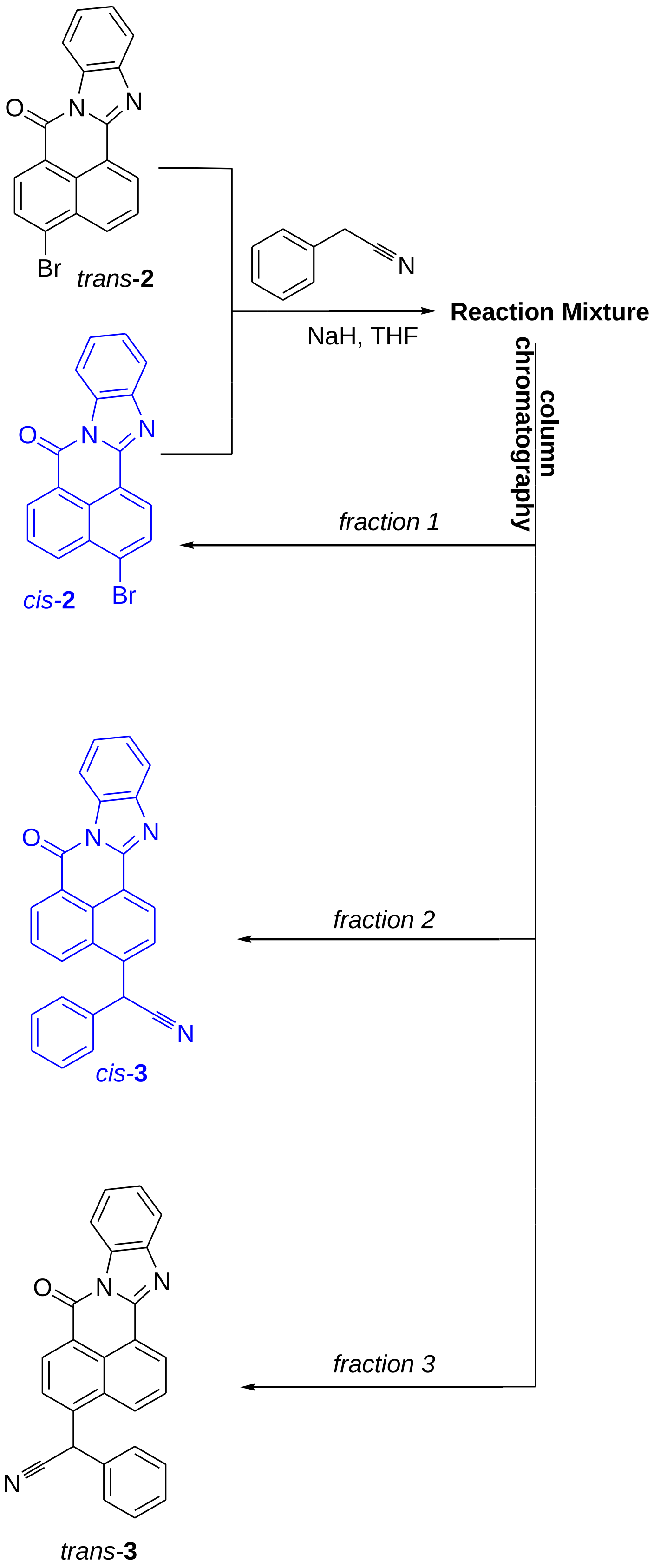

Synthesis of 4-(2-phenylacetonitrile)-7*H*-benz[*de*]benzimidazo[2,1-*a*]isoquinoline-7-one (*trans*-3), 3-(2-phenylacetonitrile)-7*H*-benz[*de*]benzimidazo[2,1-*a*]isoquinoline-7-one (*cis*-3)

and isolation of single isomer (*cis*-2): Sodium hydride (60 w % in oil, 0.42 g, 10.5 mmol) was added to a solution of phenylacetonitrile (0.30 g, 2.56 mmol) under N_2 in tetrahydrofuran (30 mL) , and the mixture was stirred at room temperature for 45 min. The reaction mixture was added with the mixture of *tran*s-**2** and *cis*-**2** (0.62 g, 1.61 mmol), stirred at room temperature for another 12 h. The reaction mixture was poured into the ice water (50 mL), subsequently dropped the hydrochloric acid until PH = 2~3, then extracted with dichloromethane (20 mL × 3), finally the organic layer was washed with brine, dried with Na_2SO_4 and filtered. After concentration of solvent, the residue was purified by chromatography with silica gel to obtain the unreactive *cis*-**2** (0.18 g, recrystallization twice from toluene), the target compounds *trans*-**3** (0.25 g, 38 %) and *cis*-**3** (0.12 g, 19 %). Moreover, the product *cis*-**3** (0.52 g, 44 %) was further synthesized by the pure *cis*-**2** (1.05 g, 3.02 mmol) with phenylacetonitrile (0.53 g, 4.53 mmol) based on the above-mentioned procedures.

3-bromo-7*H*-benz[*de*]benzimidazo[2,1-*a*]isoquinoline-7-ones (*cis*-2): ^{1}H NMR (500 MHz, $CDCl_3$) δ 7.47-7.49 (m, 2H), 7.85-7.91 (m, 2H), 8.06 (d, J = 8.0 Hz, 1H), 8.50-8.52 (m, 1H), 8.64 (d, J = 8.0 Hz, 1H), 8.65 (dd, J_1 = 8.0 Hz, J_2 = 1.0 Hz, 1H), 8.81 (dd, J_1 = 7.0 Hz, J_2 = 1.0 Hz, 1H).

4-(2-phenylacetonitrile)-7*H*-benz[*de*]benzimidazo[2,1-*a*]isoquinoline-7-one (*trans*-3): mp 254.4-256.8 °C; ^{1}H NMR (500 MHz, DMSO-d_6) δ 6.90 (s, 1H, C-H), 7.36-7.43 (m, 1H), 7.45 (dd, J_1 = 7.5 Hz, J_2 = 8.0 Hz, 2H), 7.49-7.51 (m, 4H, Ar-H), 7.87-7.89 (m, 1H), 7.96 (dd, J_1 = 7.5 Hz, J_2 = 8.5 Hz, 1H), 8.15 (d, J = 7.5 Hz, 1H), 8.42-8.44 (m, 1H), 8.50 (d, J = 8.5 Hz, 1H), 8.77 (d, J = 7.0 Hz, 1H), 8.80 (d, J = 7.5 Hz, 1H); ^{13}C NMR (100 MHz, $CDCl_3$) δ 159.9, 149.0, 143.9, 138.8, 134.2, 131.8, 131.3, 129.6, 129.6, 129.0, 128.3, 127.9, 127.8, 127.3, 127.0, 126.1, 125.8, 124.2, 121.8, 120.2, 118.7, 115.9, 40.3; IR (KBr, cm^{-1}): ν_{max} = 3058 (C-H) , 2244 (C≡N) , 1703 (C=O), 1610, 1596, 1548, 1449, 1359, 1322, 1231, 938, 778, 765, 755, 702 cm^{-1} ; HRMS-ESI (m/z): [M + H]$^+$ Calcd for $C_{26}H_{16}N_3O$ 386.12934, Found 386.13333.

3-(2-phenylacetonitrile)-7*H*-benz[*de*]benzimidazo[2,1-*a*]isoquinoline-7-one (*cis*-3): mp 258.7 - 258.9 °C; ^{1}H NMR (500 MHz, DMSO-d_6), δ 6.86 (s, 1H, C-H), 7.35-7.38 (m, H), 7.44(t, J = 7.0 Hz, 2H), 7.49-7.50 (m, 4H, Ar-H), 7.89 (s, 1H), 8.00 (dd, J_1 = 7.5 Hz, J_2 = 8.0 Hz, 1H), 8.08 (d, J = 7.5 Hz, 1H), 8.42 (s, 1H), 8.65 (d, J = 8.5 Hz, 1H), 8.71 (d, J = 6.5 Hz, 1H), 8.85 (d, J = 7.5 Hz, 1H); ^{13}C NMR (100 MHz, DMSO-d_6), δ 160.5, 149.2, 143.9, 136.8, 136.0, 132.0, 131.8, 131.5, 129.9, 129.5, 128.9, 128.4, 128.3, 128.2, 127.9, 127.0, 126.1, 125. 8, 124.3, 121.5, 120.4, 115.7, 55.4, 38.9; IR (KBr, cm^{-1}): ν_{max} = 2878 (C-H), 2242 (C≡N), 1701 (C=O), 1586, 1609, 1596, 1548, 1448, 1359, 1322, 1231, 926, 769, 755, 742, 696 cm^{-1}; HRMS-ESI (m/z): [M+H]$^+$ Calcd for $C_{26}H_{16}N_3O$ 386.12934, Found 386.13342.

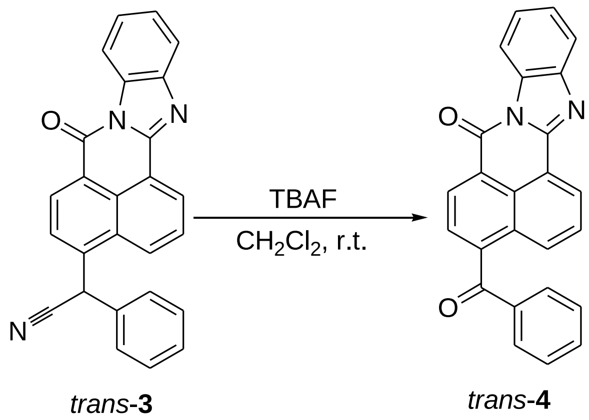

Synthesis of 4-benzoyl-7*H*-benz[*de*]benzimidazo[2,1-*a*]isoquinoline-7-one (*trans*-4): The tetrabutylammonium fluoride (98 %, 0.08 g, 0.3 mmol) was added into the mixture of compound *trans*-**3** (0.06 g, 0.15 mmol) and dichloromethane (20 mL), and stirred at room temperature. After the completion of reaction monitored by TLC, the reaction liquid was evaporated to dryness under reduced pressure. The residue was purified by chromatography with silica gel to obtain the target compound *trans*-**4** (0.05 g, 87 %). mp. 235.4-235.6 °C; ^{1}H NMR (500 MHz, DMSO-d_6), 7.53 (m, 2H), 7.62 (dd, J_1 = 7.0 Hz, J_2 = 8.0 Hz, 2H), 7.77 (t, J = 7.0 Hz, 1H), 7.85 (d, J = 7.5 Hz, 2H), 7.93 (dd, J_1 = 7.5 Hz, J_2 = 8.0 Hz, 2H), 8.04 (d, J = 7.0 Hz, 1H), 8.15 (d, J = 8.5 Hz, 1H), 8.47 (m, 1H), 8.80 (d, J = 7.5 Hz, 1H), 8.83 (d, J = 7.0 Hz, 1H); ^{13}C NMR (100 MHz, $CDCl_3$), δ 196.4, 160.1, 149.1, 143.9, 143.4, 134.3, 130.5, 130.3, 129.7, 128.9, 128.4, 127.6, 127.0, 126.1, 125.7, 121.0, 120.1, 115.9; IR (KBr, cm^{-1}): ν_{max} = 3057, 1702(C=O), 1655, 1613, 1595, 1579, 1552, 1448, 1366, 1348, 1269, 1127, 1160, 908, 884, 779, 762, 748 cm^{-1}; HRMS-ESI (m/z): [M+H]$^+$ Calcd for $C_{25}H_{15}N_2O_2$ 375.11335, Found 375.11549.

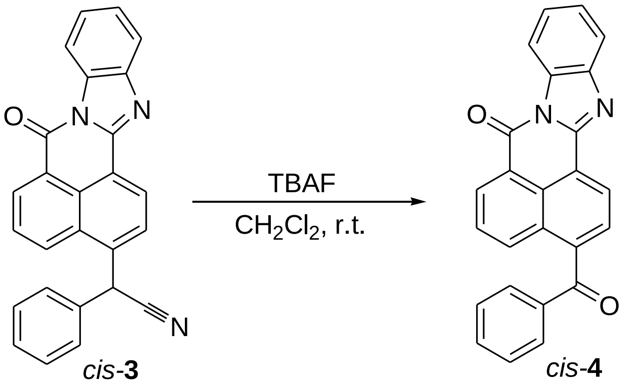

Synthesis of 3-benzoyl-7*H*-benz[*de*]benzimidazo[2,1-*a*]isoquinoline-7-one (*cis*-4): The tetrabutylammonium fluoride (98 %, 0.08 g, 0.3 mmol) was added into the mixture of compound *cis*-**3** (0.06 g, 0.15 mmol) and dichloromethane (20 mL), and stirred at room temperature. After the completion of reaction monitored by TLC, the reaction liquid was evaporated to dryness under reduced pressure. The residue was purified by chromatography with silica gel to obtain the target compound *cis*-**4** (0.04 g, 70 %). mp 258.3-259 °C ; ^{1}H NMR (500 MHz, DMSO-d_6) , 7.54 (m, 2H), 7.61 (t, J = 7.5 Hz, 2H), 7.77 (dd, J_1 = 6.0 Hz, J_2 = 7.5 Hz, 2H), 7.87 (d, J = 8.0 Hz, 2H), 7.94 (d, J = 7.5 Hz, 2H), 7.98 (dd, J_1 = 7.5 Hz, J_2 = 8.0 Hz,, 1H), 8.01 (d, J = 7.5 Hz, 1H), 8.42 (d, J = 8.5 Hz, 1H), 8.48 (d, J = 7.5 Hz, 1H), 8.78 (d, J = 7.0 Hz, 1H), 8.85 (d, J = 7.5 Hz, 1H); ^{13}C NMR (100 MHz, DMSO-d_6) , δ 196.5, 160.5, 149.1, 144.0, 139.6, 137.5, 134.7, 133.1, 132.1, 130.6, 129.8, 129.5, 128.9, 127.4, 126.2, 126.1, 125.9, 123.9, 123.0, 120.6, 115.8; IR (KBr, cm^{-1}): ν_{max} = 3057, 1699 (C=O), 1655, 1608, 1596, 1580, 1546, 1505, 1449, 1389, 1355, 1307, 1273, 1230, 1099, 930, 919, 882, 857, 802, 768, 761, 710, 692, 670 cm^{-1}; HRMS-ESI (m/z): [M + H]$^+$ Calcd for $C_{25}H_{15}N_2O_2$ 375.11335, Found 375.11564.

Reference:

(1) K, Nakaya.; T, Tanaka.; Y, Shirataki.; H, Shiozaki.; K, Funabiki.; K, Shibata.; M, Matsui. *Bull. Chem. Soc. Jpn.* **2001**, *74*, 173–177.

(2) J, Lee.; S. L.-C, Hsu. *Polymer*, **2009**, *50*, 5668–5674.

(3) M, Verma.; V, Luxami.; K, Paul. *European Journal of Medicinal Chemistry*, **2013**, *68*, 352–360.

(4) W, Jiang.; J, Tang.; Q, Qi.; Y, Sun.; H, Ye.; D, Fu. *Dyes and Pigments*, **2009**, *80*, 279–286.

(5) W, Zhu.; R .Yao.; H, Tian. *Dyes and Pigments*, **2002**, *54*, 147–154.

(6) J, Chen.; C, Liu.; J, Zhang.; W, Ding.; M, Zhou.; F, Wu. *Chem. Commun*. **2013**, *49*, 10814–10816.

4. ^{1}H-NMR spectrum of the compound *cis*-2 and the mixture of *trans*-2 and *cis*-2.

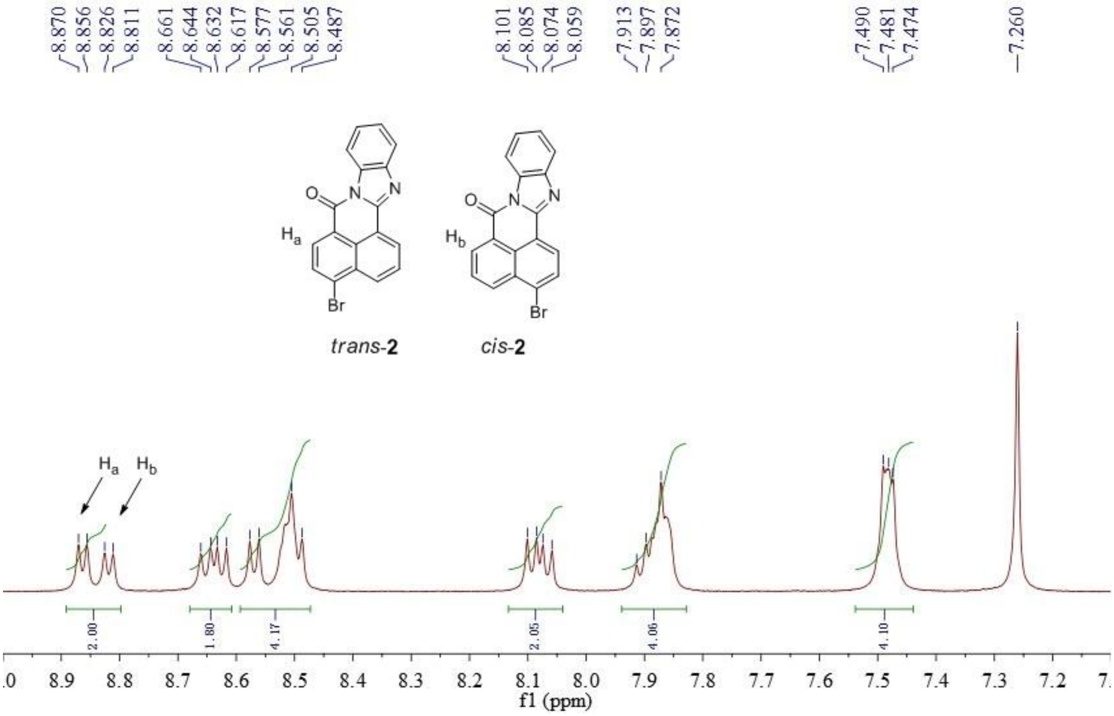

Figure S1. ^{1}H-NMR ($CDCl_3$, 500 MHz) spectrum of the mixture of *trans*-**2** and *cis*-**2**.

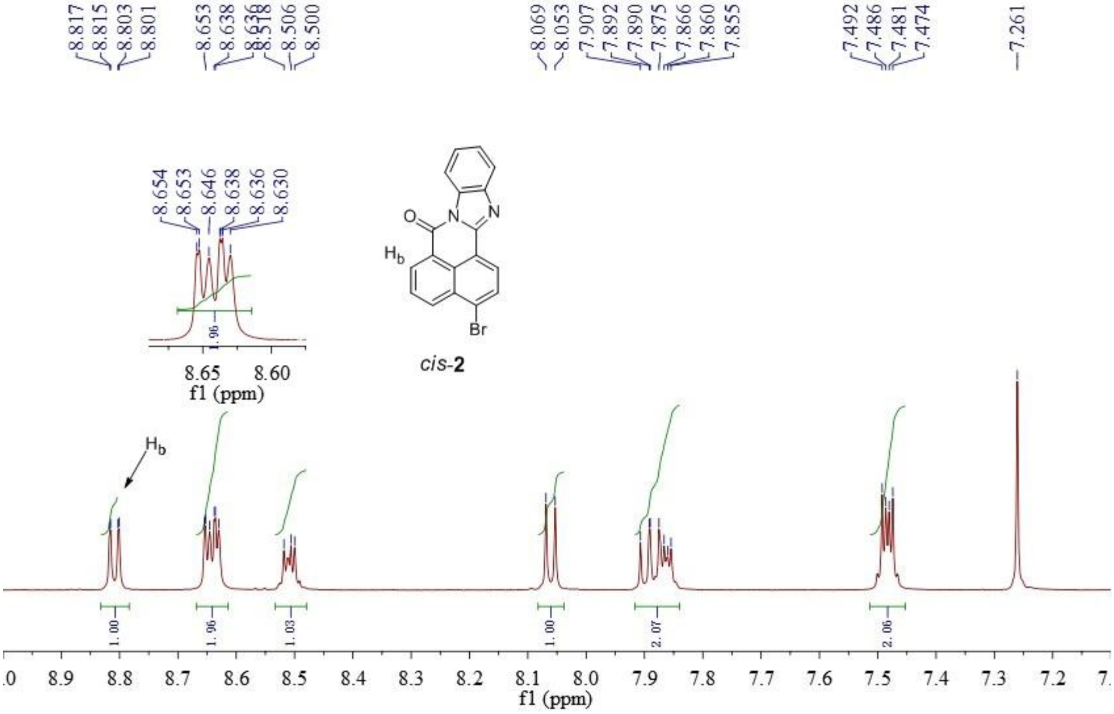

Figure S2. ^{1}H-NMR ($CDCl_3$, 500 MHz) spectrum of compound *cis*-**2**

5. ^{1}H-NMR, ^{13}C-NMR, IR and HRMS-ESI spectrum of the compound *trans*-3.

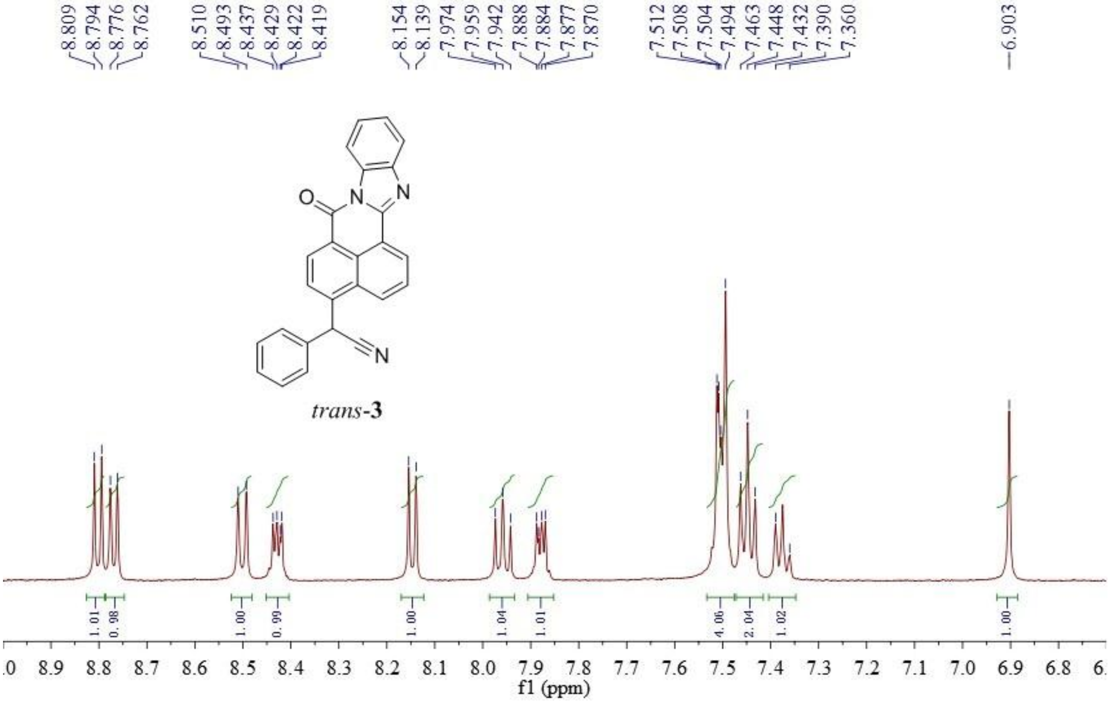

Figure S3. ^{1}H-NMR (DMSO-d_6, 500 MHz) spectrum of compound *trans*-**3**

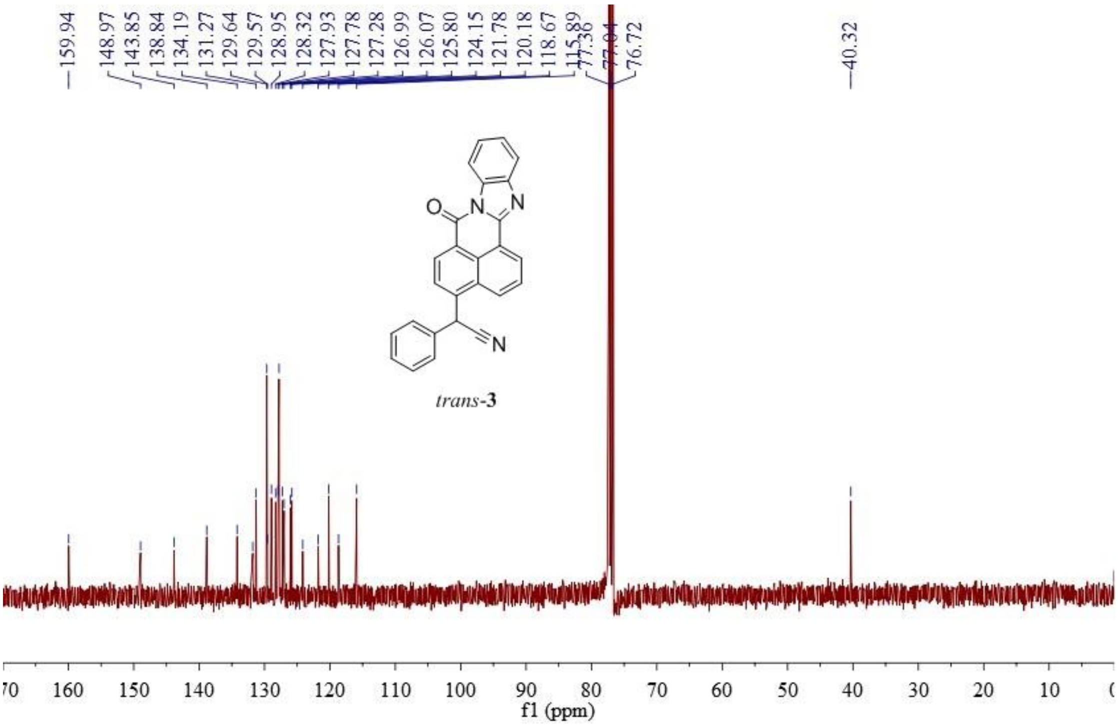

Figure S4.^{13}C-NMR (CDCl$_3$, 400 MHz) spectrum of compound *trans*-**3**

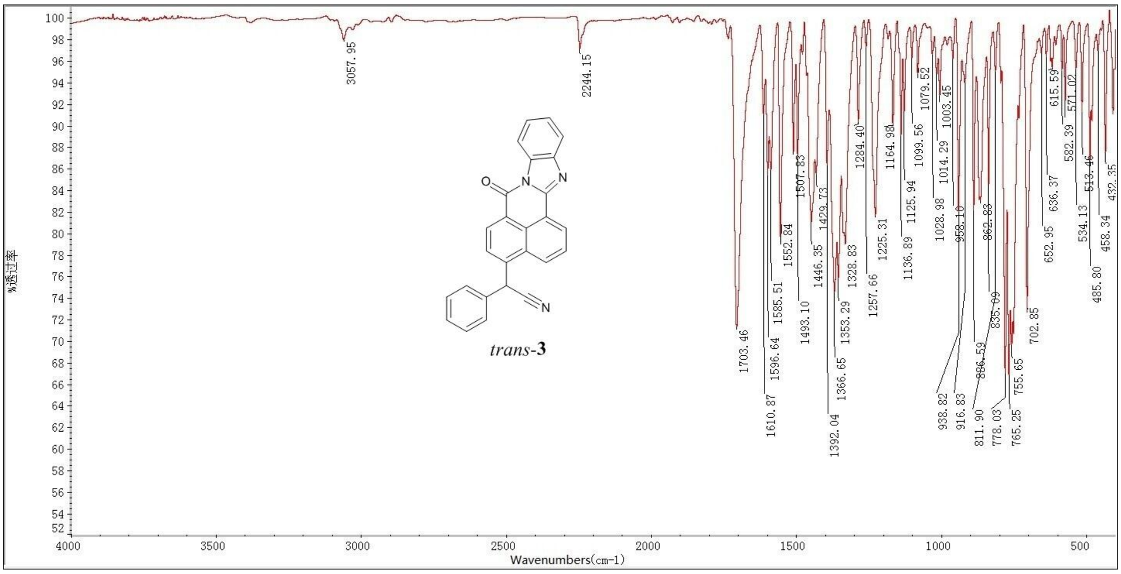

Figure S5. IR spectrum of compound *trans*-**3**

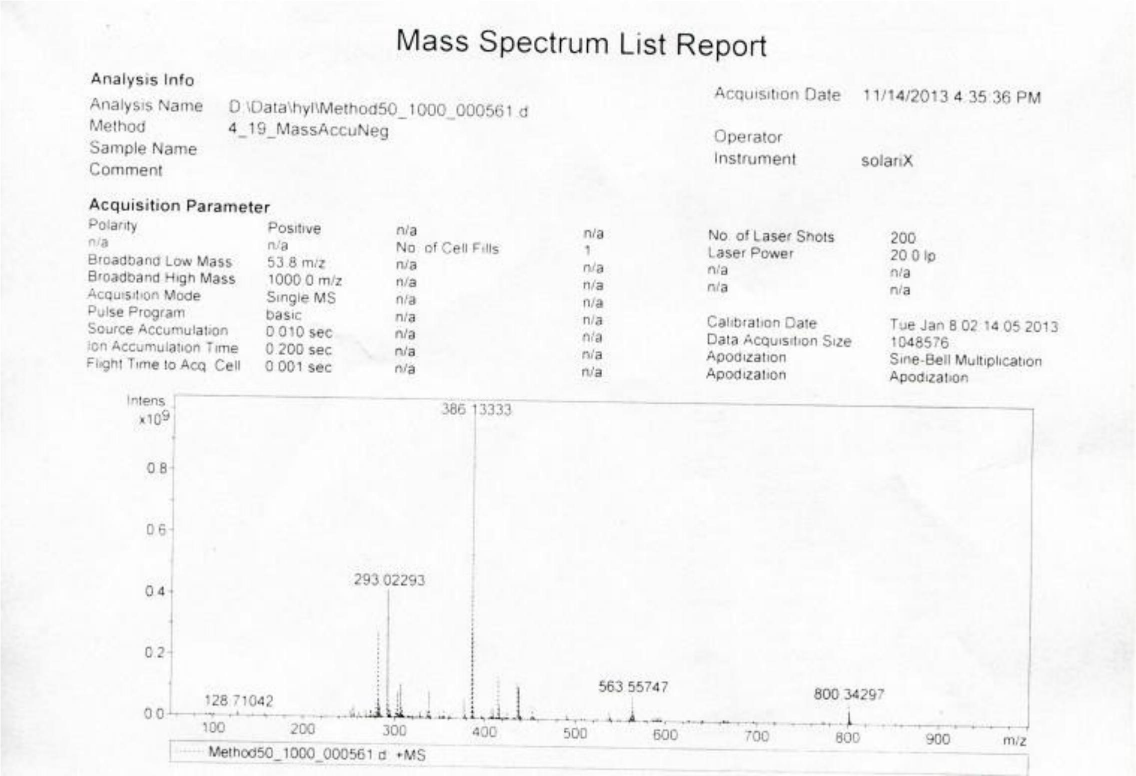

Mass Spectrum List Report

Analysis Info

Analysis Name D:\Data\hyl\Method50_1000_000561.d

Method 4_19_MassAccuNeg

Sample Name

Comment

Acquisition Date 11/14/2013 4:35:36 PM

Operator

Instrument solariX

Acquisition Parameter

Polarity	Positive	n/a	n/a	No. of Laser Shots	200
n/a	n/a	No. of Cell Fills	1	Laser Power	20.0 lp
Broadband Low Mass	53.8 m/z	n/a	n/a	n/a	n/a
Broadband High Mass	1000.0 m/z	n/a	n/a	n/a	n/a
Acquisition Mode	Single MS	n/a	n/a		
Pulse Program	basic	n/a	n/a	Calibration Date	Tue Jan 8 02:14:05 2013
Source Accumulation	0.010 sec	n/a	n/a	Data Acquisition Size	1048576
Ion Accumulation Time	0.200 sec	n/a	n/a	Apodization	Sine-Bell Multiplication
Flight Time to Acq. Cell	0.001 sec	n/a	n/a	Apodization	Apodization

Figure S6. HRMS-ESI mass spectrum of compound *trans*-**3**

6. ^{1}H-NMR, ^{13}C-NMR, IR and HRMS-ESI spectrum of the compound *trans*-4.

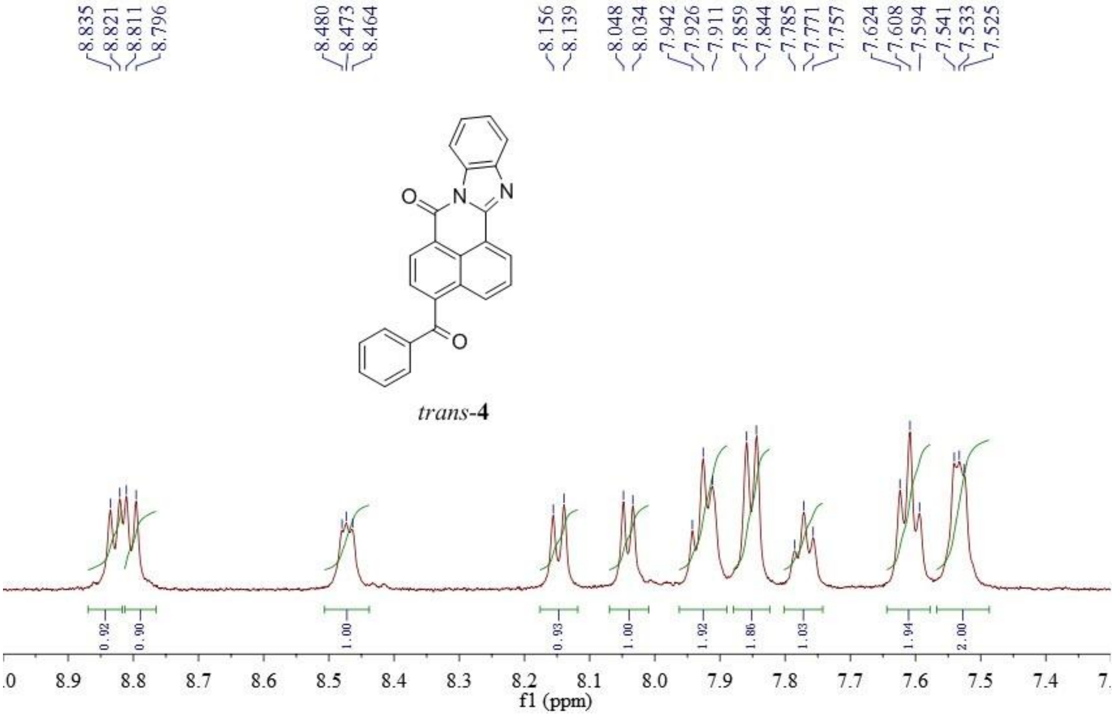

Figure S7. ^{1}H-NMR (DMSO-d_6, 500 MHz) spectrum of compound *trans*-**4**

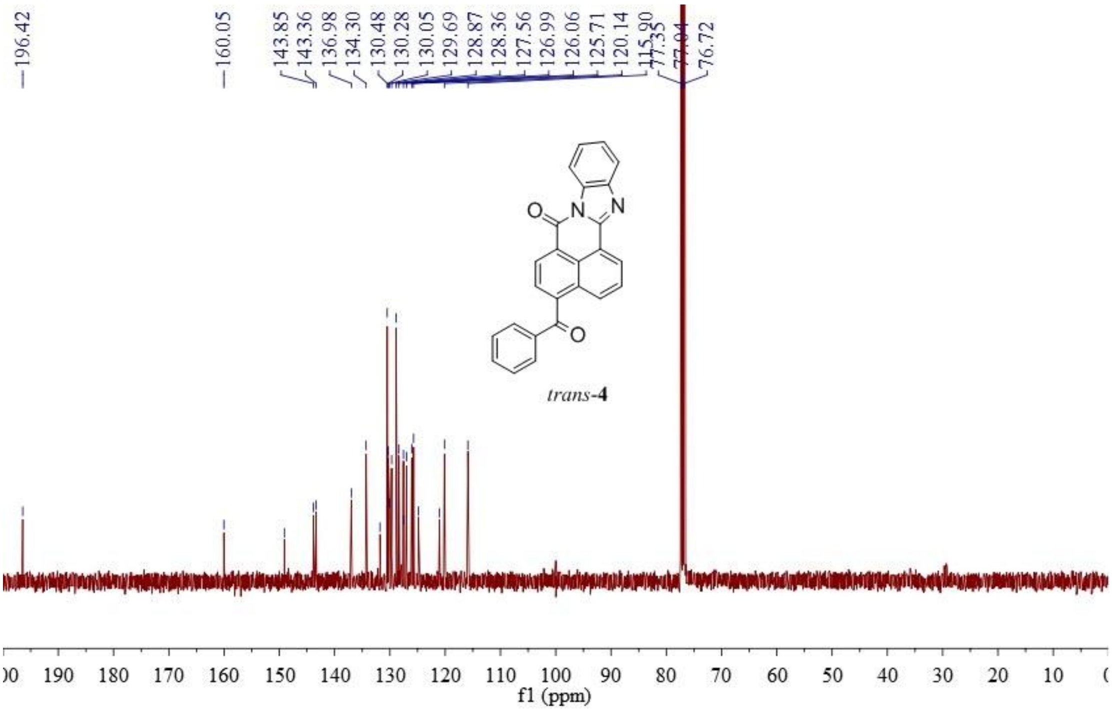

Figure S8. ^{13}C-NMR (CDCl$_3$, 400 MHz) spectrum of compound *trans*-**4**

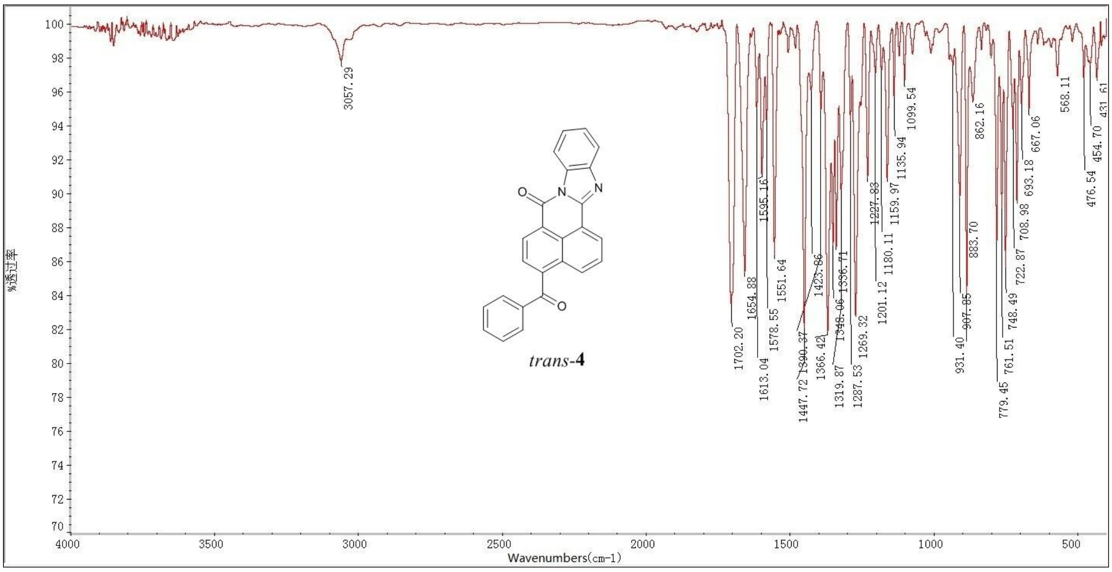

Figure S9. IR spectrum of compound *trans*-**4**

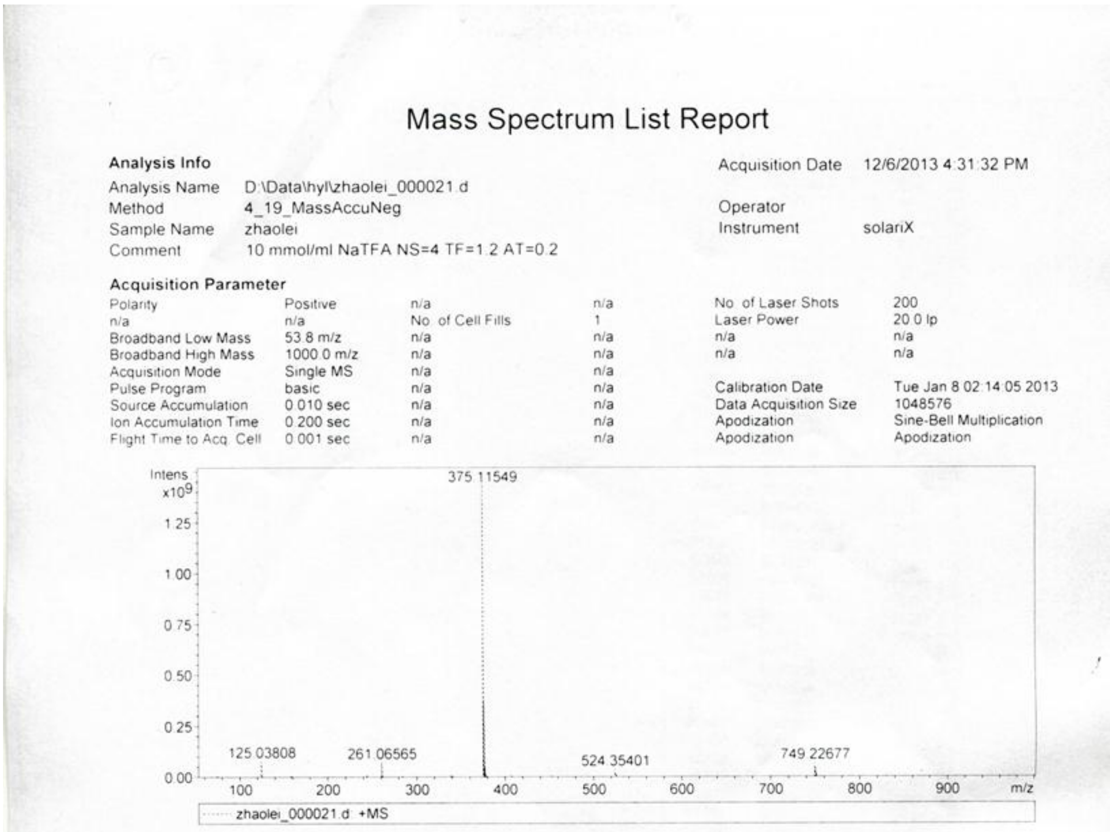

Mass Spectrum List Report

Analysis Info

Analysis Name	D:\Data\hyl\zhaolei_000021.d	Acquisition Date	12/6/2013 4:31:32 PM
Method	4_19_MassAccuNeg		
Sample Name	zhaolei	Operator	
Comment	10 mmol/ml NaTFA NS=4 TF=1.2 AT=0.2	Instrument	solariX

Acquisition Parameter

Polarity	Positive	n/a	n/a	No. of Laser Shots	200
n/a	n/a	No. of Cell Fills	1	Laser Power	20.0 lp
Broadband Low Mass	53.8 m/z	n/a	n/a	n/a	n/a
Broadband High Mass	1000.0 m/z	n/a	n/a	n/a	n/a
Acquisition Mode	Single MS	n/a	n/a		
Pulse Program	basic	n/a	n/a	Calibration Date	Tue Jan 8 02:14:05 2013
Source Accumulation	0.010 sec	n/a	n/a	Data Acquisition Size	1048576
Ion Accumulation Time	0.200 sec	n/a	n/a	Apodization	Sine-Bell Multiplication
Flight Time to Acq. Cell	0.001 sec	n/a	n/a	Apodization	Apodization

Figure S10. HRMS-ESI mass spectrum of compound *trans*-**4**

7. ^{1}H-NMR, ^{13}C-NMR, IR and HRMS-ESI spectrum of the compound *cis*-3.

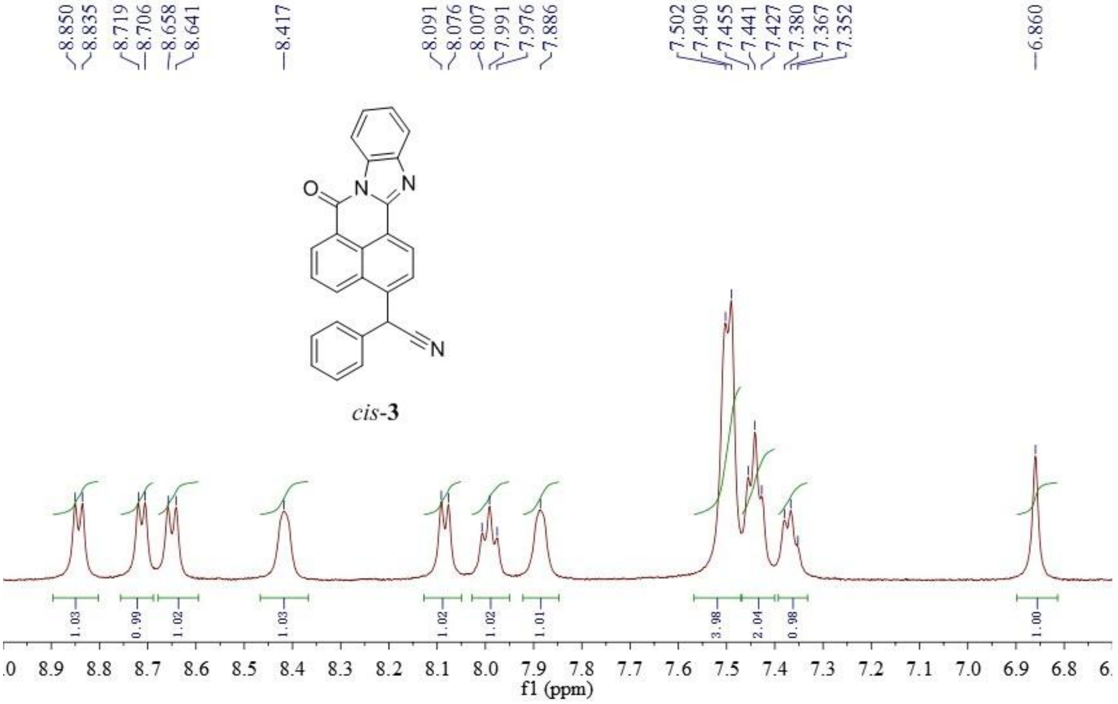

Figure S11. ^{1}H-NMR (DMSO-d_6, 500 MHz) spectrum of compound *cis*-**3**

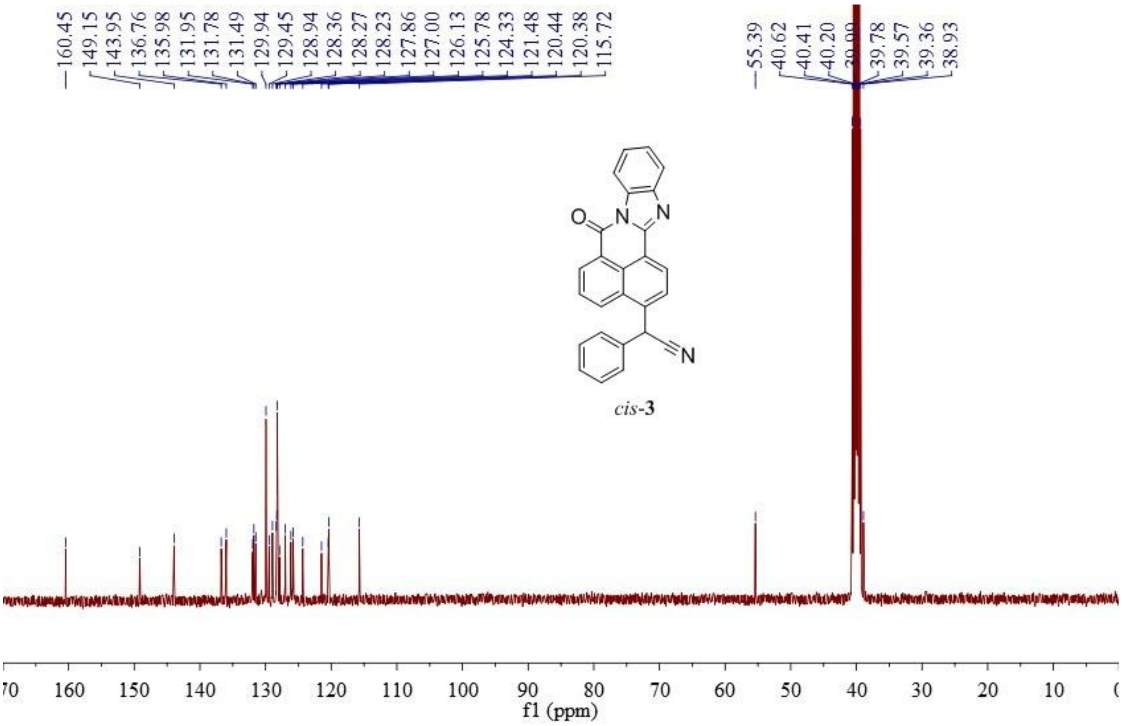

Figure S12. ^{13}H-NMR (DMSO-d_6, 400 MHz) spectrum of compound *cis*-**3**

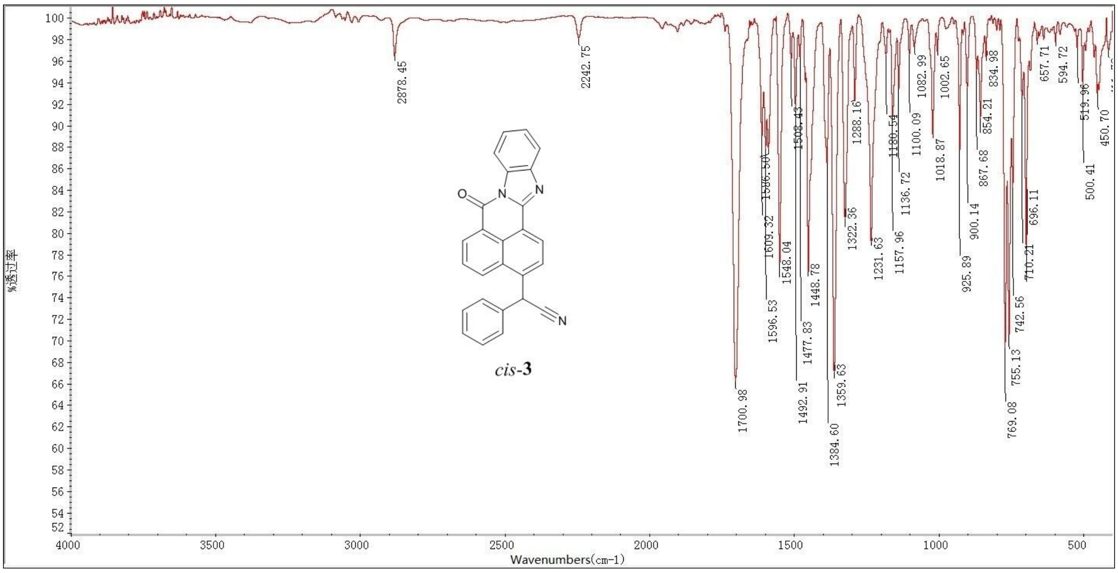

Figure S13. IR spectrum of compound *cis*-**3**

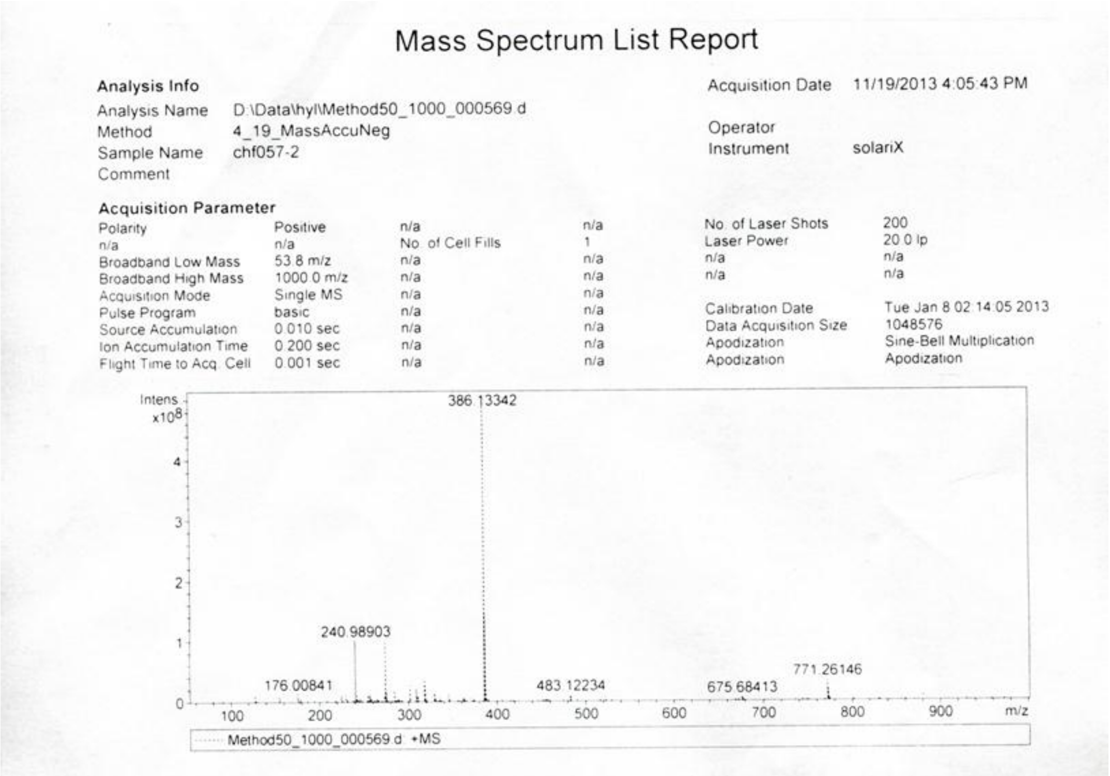

Mass Spectrum List Report

Analysis Info

Analysis Name D:\Data\hyl\Method50_1000_000569.d
Method 4_19_MassAccuNeg
Sample Name chf057-2
Comment

Acquisition Date 11/19/2013 4:05:43 PM

Operator
Instrument solariX

Acquisition Parameter

Polarity	Positive	n/a	n/a	No. of Laser Shots	200
n/a	n/a	No. of Cell Fills	1	Laser Power	20.0 lp
Broadband Low Mass	53.8 m/z	n/a	n/a	n/a	n/a
Broadband High Mass	1000.0 m/z	n/a	n/a	n/a	n/a
Acquisition Mode	Single MS	n/a	n/a		
Pulse Program	basic	n/a	n/a	Calibration Date	Tue Jan 8 02:14:05 2013
Source Accumulation	0.010 sec	n/a	n/a	Data Acquisition Size	1048576
Ion Accumulation Time	0.200 sec	n/a	n/a	Apodization	Sine-Bell Multiplication
Flight Time to Acq. Cell	0.001 sec	n/a	n/a	Apodization	Apodization

Figure S14. HRMS-ESI mass spectrum of compound *cis*-**3**

8. ^{1}H-NMR, ^{13}C-NMR, IR and HRMS-ESI spectrum of the compound *cis*-4.

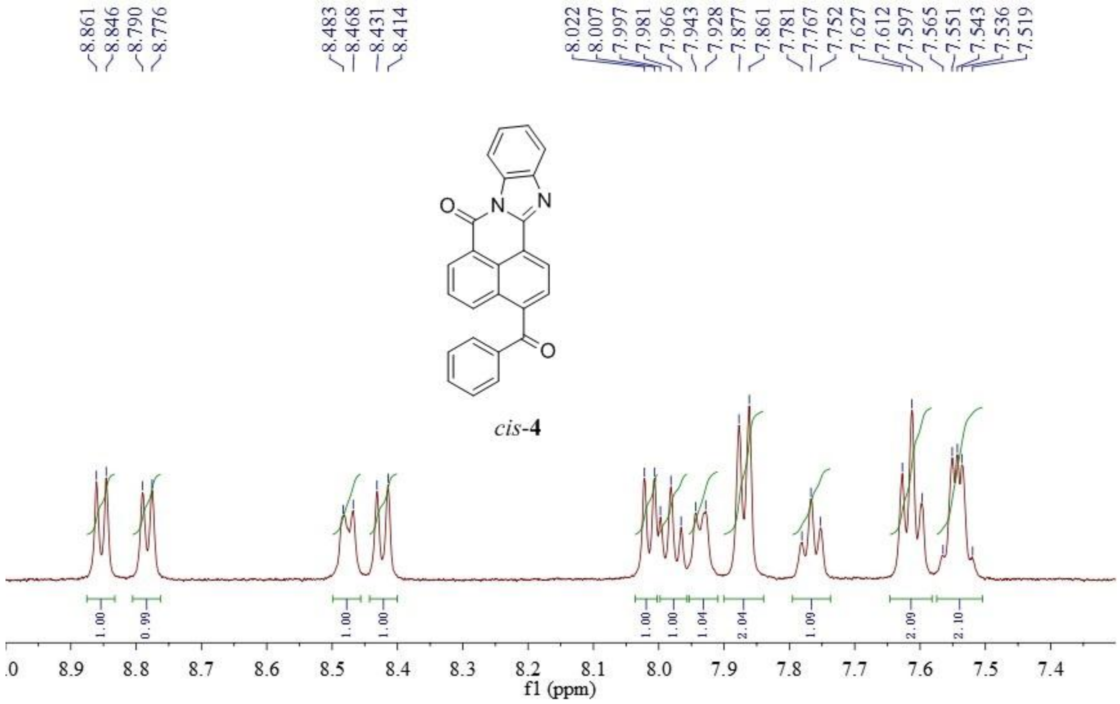

Figure S15. ^{1}H-NMR (DMSO-d_6, 400 MHz) spectrum of compound *cis*-**4**

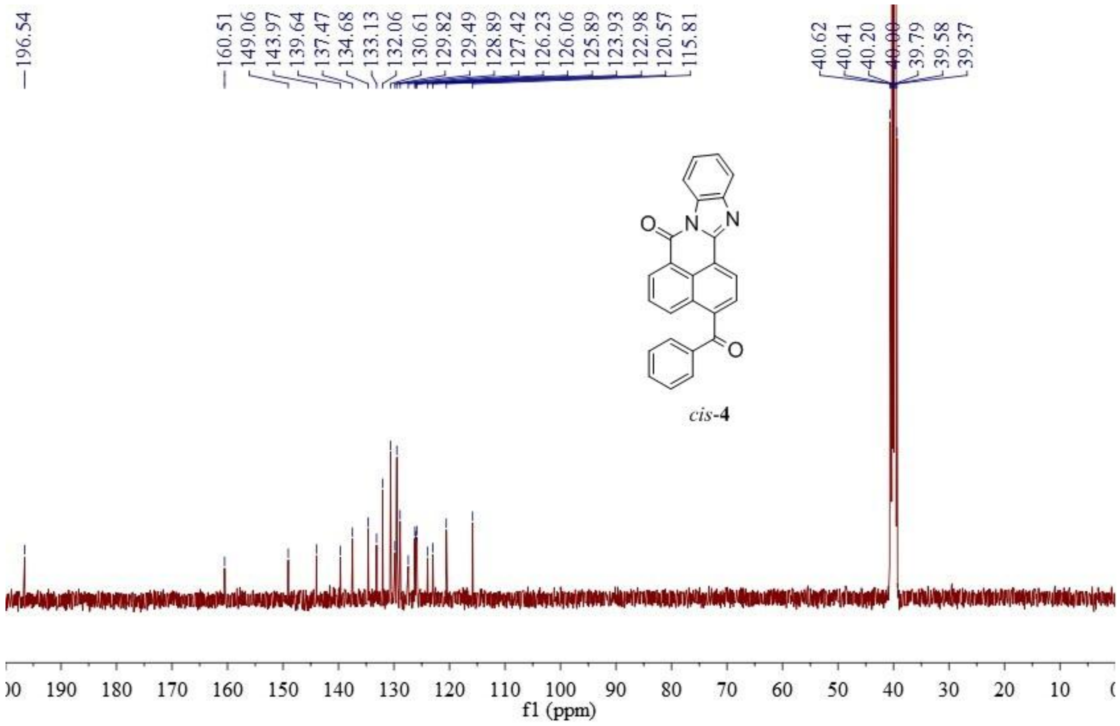

Figure S16. ^{13}C-NMR (DMSO-d_6, 400 MHz) spectrum of compound *cis*-**4**

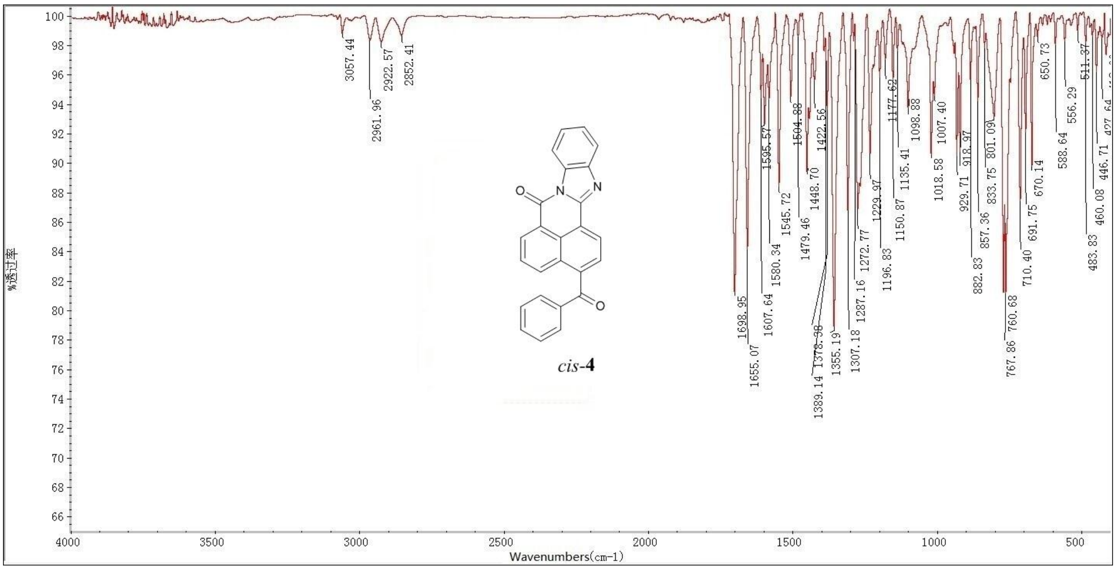

Figure S17. IR spectrum of compound *cis*-**4**

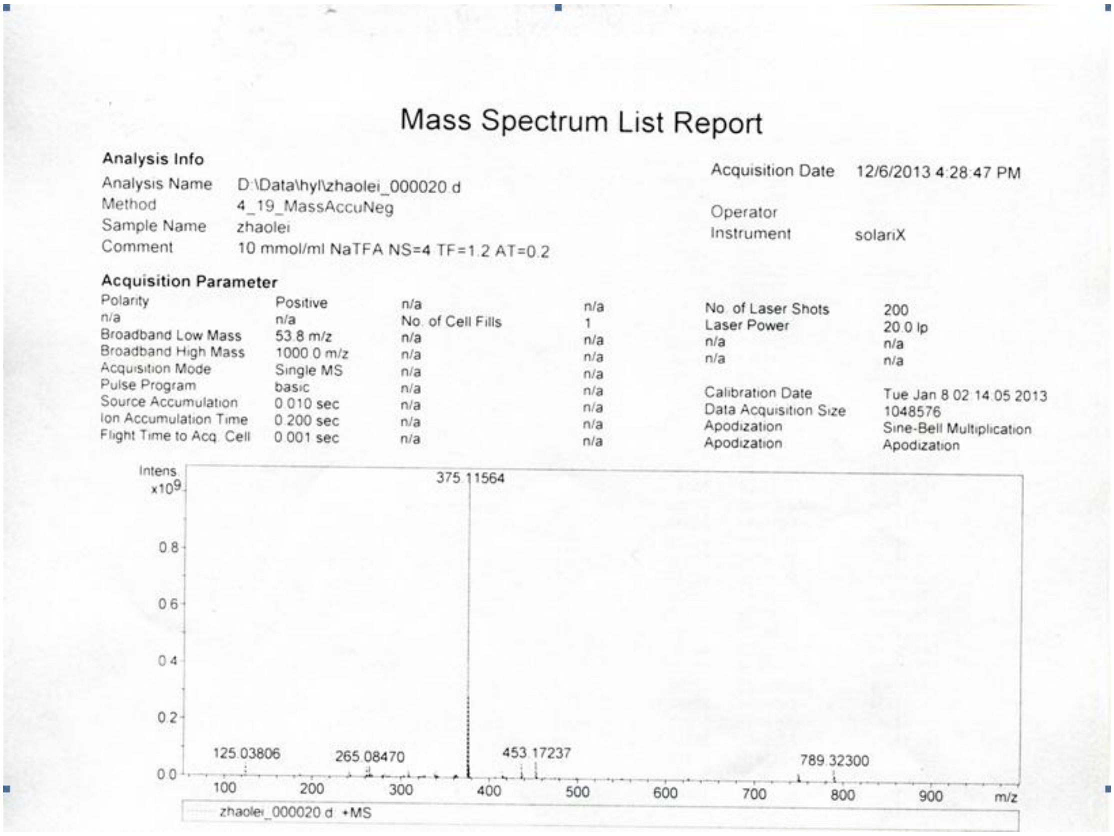

Mass Spectrum List Report

Analysis Info

Analysis Name	D:\Data\hyl\zhaolei_000020.d	Acquisition Date	12/6/2013 4:28:47 PM
Method	4_19_MassAccuNeg		
Sample Name	zhaolei	Operator	
Comment	10 mmol/ml NaTFA NS=4 TF=1.2 AT=0.2	Instrument	solariX

Acquisition Parameter

Polarity	Positive	n/a	n/a	No. of Laser Shots	200
n/a	n/a	No. of Cell Fills	1	Laser Power	20.0 lp
Broadband Low Mass	53.8 m/z	n/a	n/a	n/a	n/a
Broadband High Mass	1000.0 m/z	n/a	n/a	n/a	n/a
Acquisition Mode	Single MS	n/a	n/a		
Pulse Program	basic	n/a	n/a	Calibration Date	Tue Jan 8 02:14:05 2013
Source Accumulation	0.010 sec	n/a	n/a	Data Acquisition Size	1048576
Ion Accumulation Time	0.200 sec	n/a	n/a	Apodization	Sine-Bell Multiplication
Flight Time to Acq. Cell	0.001 sec	n/a	n/a	Apodization	Apodization

Figure S18. HRMS-ESI mass spectrum of compound *cis*-**4**

9. The absorbance detection limit of *cis*-3 and *trans*-3 with CN⁻ in CH_3CN

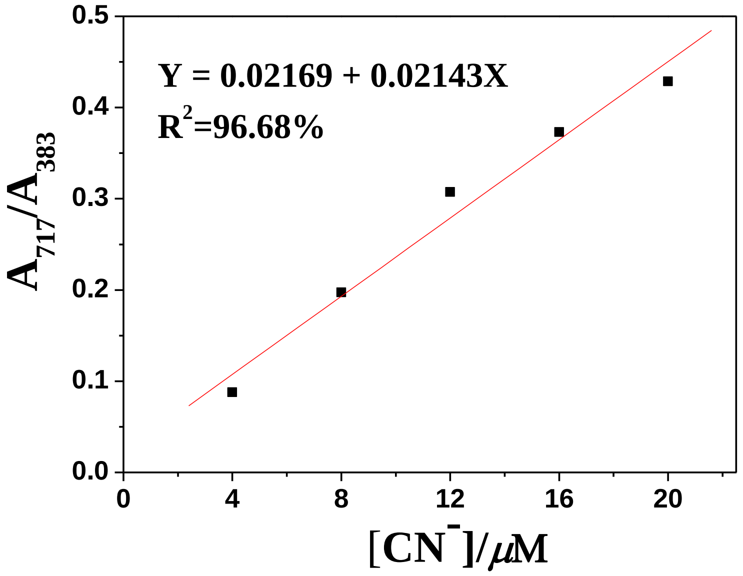

Figure S19. Absorbance intensity ratio (A_{717}/A_{383}) of *cis*-**3** (20 μM) as a function of CN⁻ concentration from 0 – 20 μM (0–1.0 equivalents)

Linear Regression for Book1_B:

Equation	Y = A + B * X	
Parameter	Value	Error
A	0.02169	0.02542
B	0.02143	0.00192
R	SD	N
0.98822	0.02423	5

Linear Equation: Y = 0.02291 * X, R = 0.99289

S= 2.143 * 10^4, K = 3, δ = 0.02423

LOD = K *δ / S = 0.81 μM

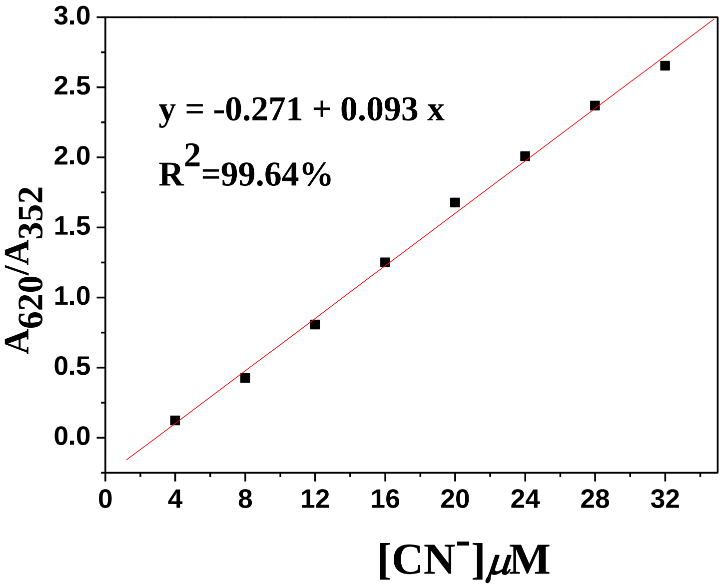

Figure S20. Absorbance intensity ratio (A_{620}/A_{352}) of *trans*-**3** (20 μM) as a function of CN^- concentration from 0- 32 μM (0–1.6 equivalents)

Linear Regression for Book1_B:

Equation	Y = A + B * X	
Parameter	Value	Error
A	-0.27198	0.04259
B	0.09365	0.00211
R	SD	N
0.99848	0.05466	8

The result of the analysis as follows:

Linear Equation: Y = - 0.27198 + 0.09365 * X, R = 0.99848

S= 9.365 * 10^4, K = 3, δ = 0.05466

LOD = K *δ / S = 1.75 μM

10. UV-vis titration of *cis*-3 and *trans*-3 with CN$^-$ in CH$_3$CN.

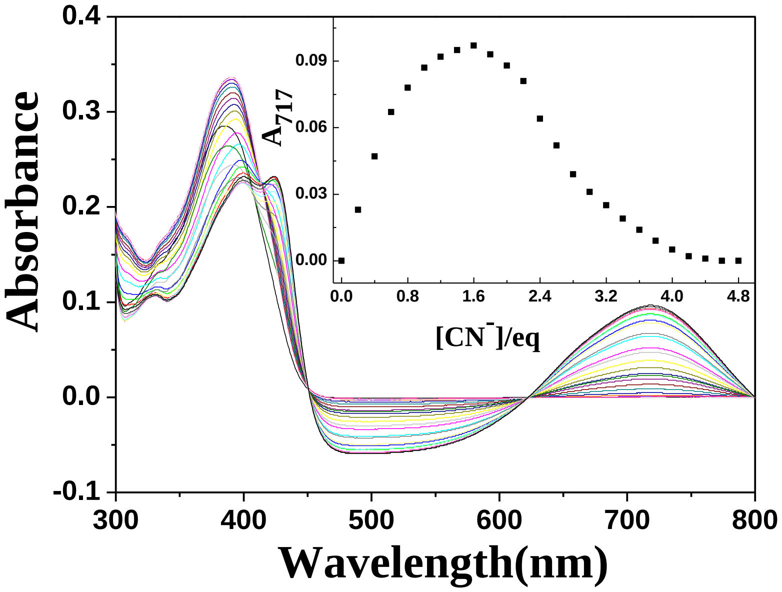

Figure S21. UV-visible spectral changes of 20 μM solution of *cis*-**3** upon titration with CN$^-$ (as its TBA salts) in CH$_3$CN;

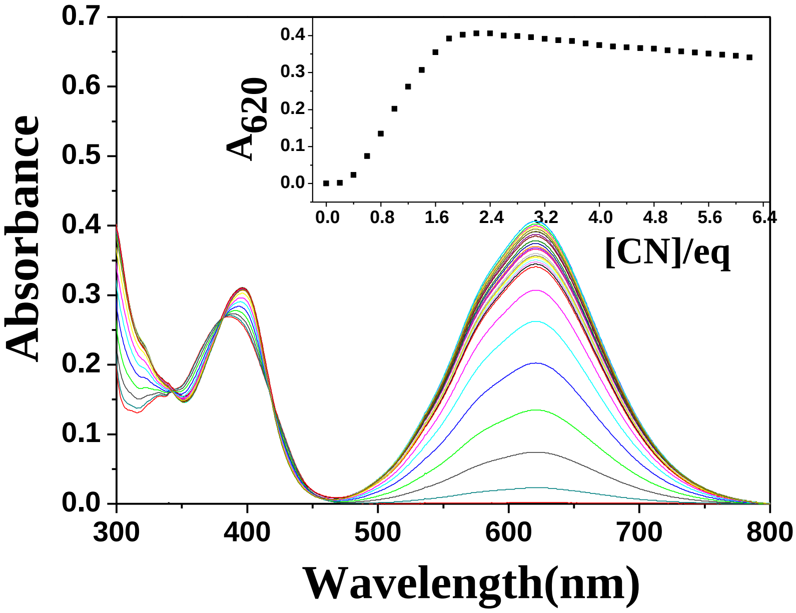

Figure 22. UV-visible spectral changes of 20 μM solution of *trans*-**3** upon titration with CN$^-$ (as its TBA salts) in CH$_3$CN;

11. UV-vis interference experiments of *trans*-3 and *cis*-3 toward CN$^-$ ions.

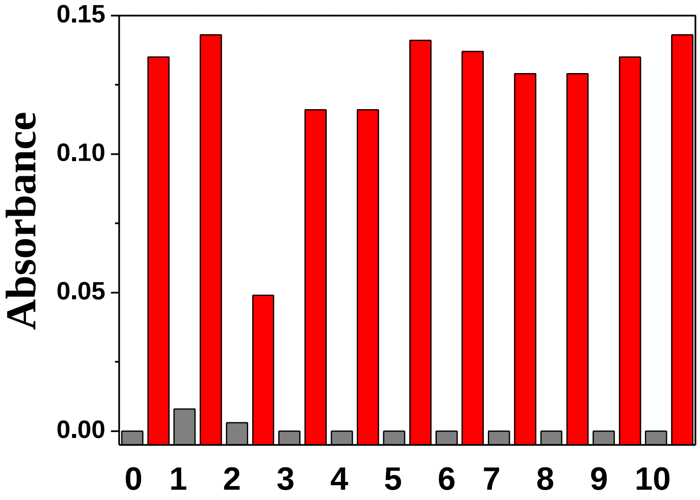

Figure S23. UV-visible spectral changes (A_{717}) of *cis*-**3** (20 μM in CH_3CN) upon addition of 1.6 equiv of CN$^-$ and 1.6 equiv of various interference anions. (the light gray bars represent the change in A_{717} from 0 to 10 : *cis*-**3** only, F$^-$, AcO$^-$, $H_2PO_4^-$, Cl$^-$, Br$^-$, I$^-$, NO_3^-, HSO_4^-, BF_4^-, ClO_4^-; the red bars represent the addition of corresponding equiv of CN$^-$ ions)

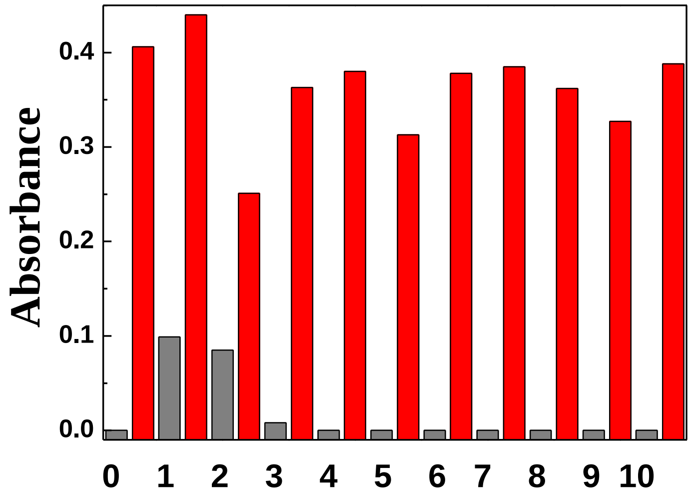

Figure S24. UV-visible spectral changes (A_{620}) of *trans*-**3** (20 μM in CH_3CN) upon addition of 2.0 equiv of CN$^-$ and 2.0 equiv of various interference anions. (the light gray bars represent the change in A_{620} from 0 to 10 : *trans*-**3** only, F$^-$, AcO$^-$, $H_2PO_4^-$, Cl$^-$, Br$^-$, I$^-$, NO_3^-, HSO_4^-, BF_4^-, ClO_4^-; the red bars represent the addition of corresponding equiv of CN$^-$ ions);

12. UV-vis titration of *trans*-3 with CN^- in CH_3CN-H_2O solution.

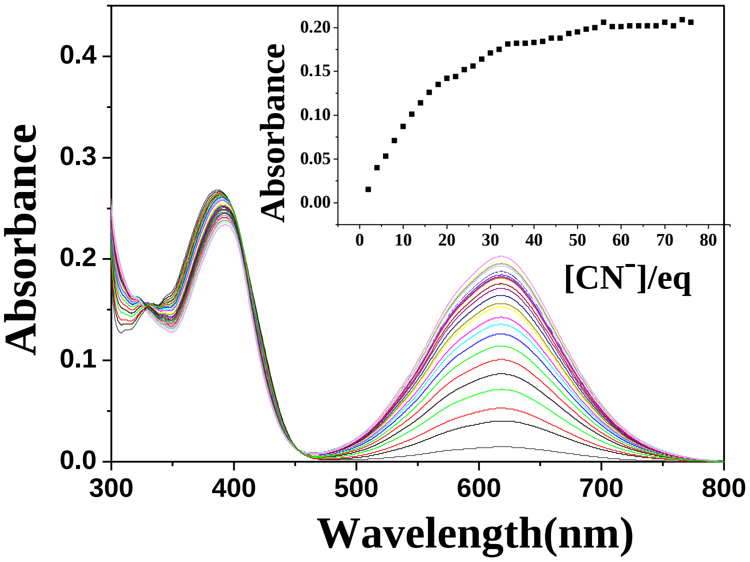

Figure S25. UV-visible spectral changes of 20 μM solution of *trans*-**3** upon titration with CN^- (as its TBA salts) in CH_3CN-H_2O (95:5, v/v) solution;

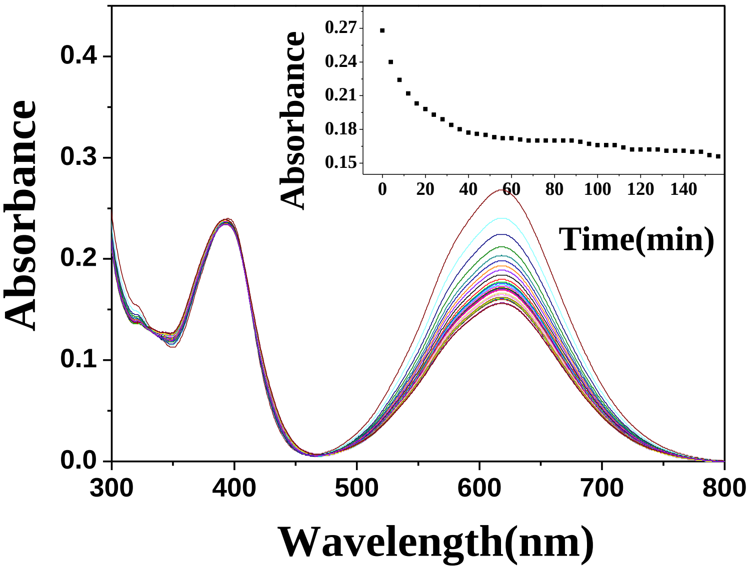

Figure S26. Time-dependence of UV-visible spectral changes of 20 μM solution of *trans*-**3** upon titration with CN^- (56 equiv) in CH_3CN-H_2O (9:5, v/v) solution;

13. UV-vis titration of compounds *cis*-3 and *trans*-3 with OH^- in CH_3CN.

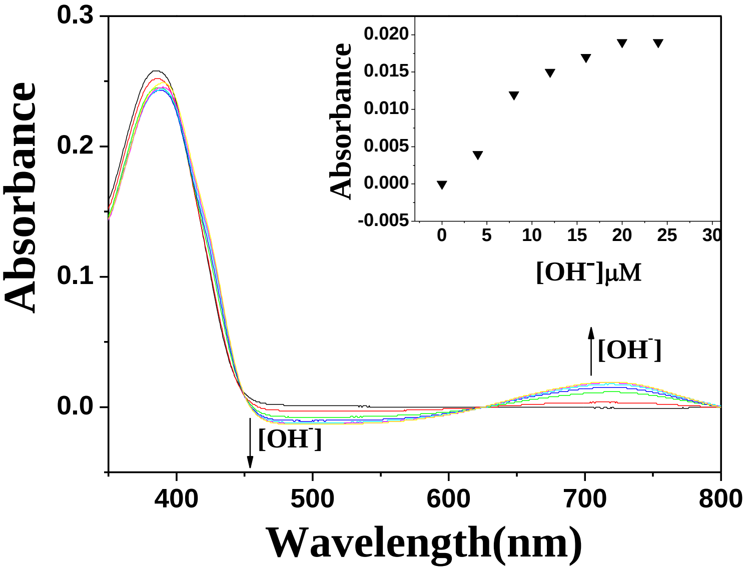

Figure S27. UV-visible titration of ***cis*-3** (20 μM) with $Bu_4N^+OH^-$ (25% aq.) in CH_3CN. Arrows show changes due to increasing concentration of OH^- (500 μM). The inset shows the absorbance at 717 nm as a function of $[OH^-]$.

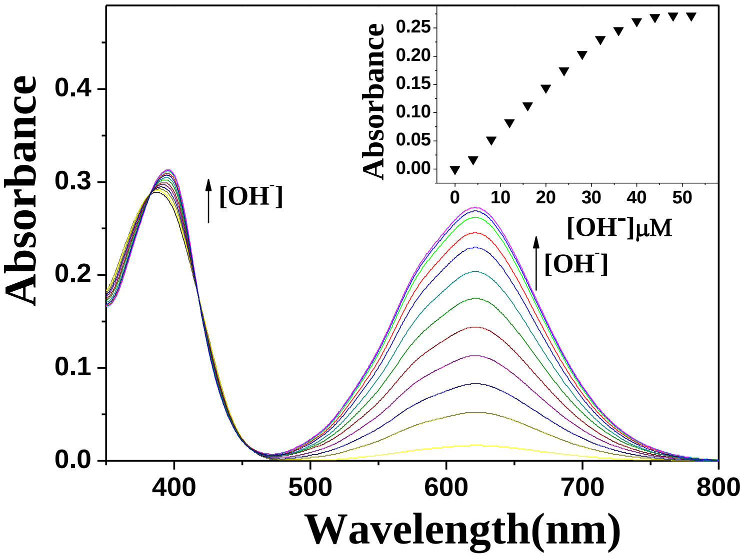

Figure S28. UV-visible titration of *trans*-**3** (20 μM) with $Bu_4N^+OH^-$ (25% aq.) in CH_3CN. Arrows show changes due to increasing concentration of OH^- (500 μM). The inset shows the absorbance at 620 nm as a function of $[OH^-]$.

14. UV-vis spectrum of selectivity of *trans*-3 with anion in CH_3CN-H_2O solution.

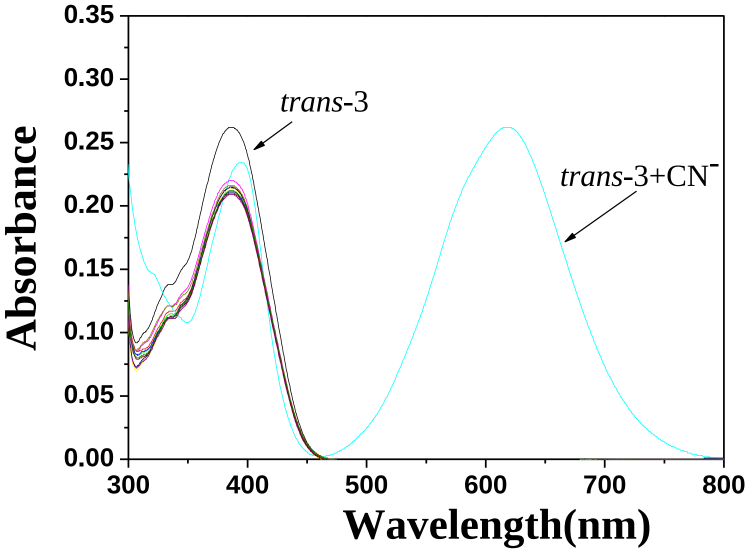

Figure S29. UV-visible spectra of 20 μM solution of *trans*-**3** in CH_3CN-H_2O (95:5, v/v) solution in the presence of 56 equiv of different anions.

15. Emission spectra of selectivity and titration of *cis*-3 and *trans*-3 with CN⁻ in CH_3CN.

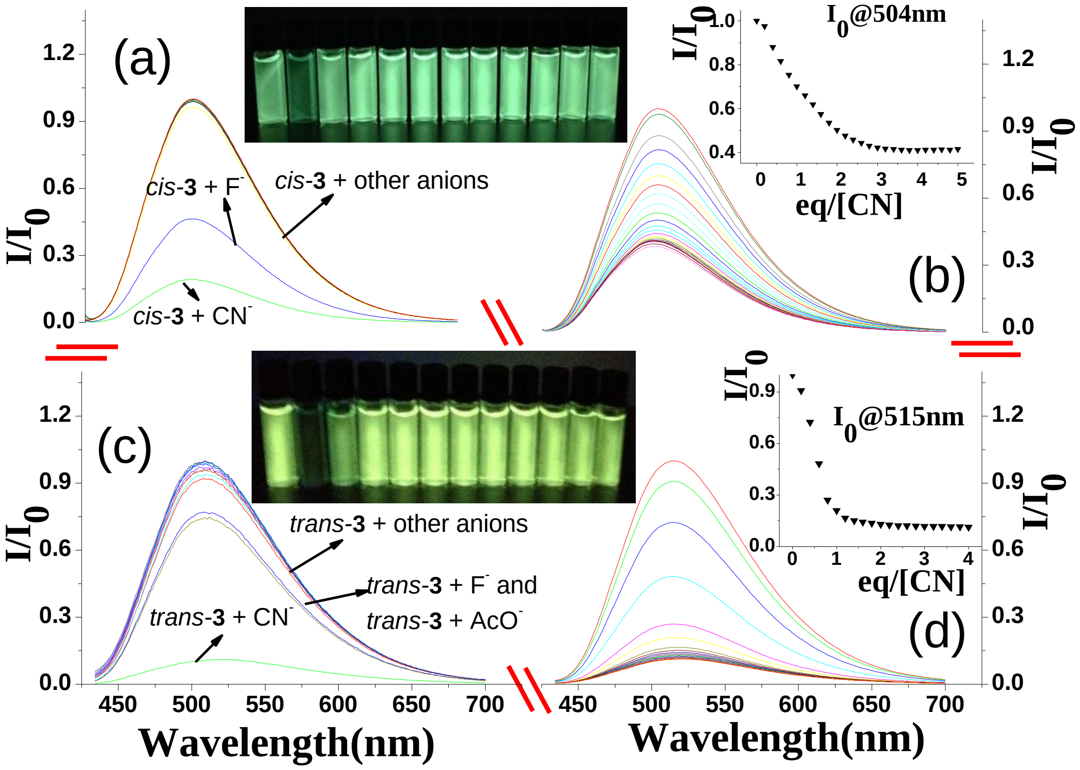

Figure S30. Emission spectra of 20 μM solution of (a) *cis*-**3** and (c) *trans*-**3** in CH_3CN in the presence of different anions (4.0 equiv for *cis*-**3** and 2.0 equiv for *trans*-**3**), Inset: from left to right: *cis*-**3**/*trans*-**3** only, CN^-, F^-, AcO^-, $H_2PO_4^-$, Cl^-, Br^-, HSO_4^-, I^-, NO_3^-, BF_4^-, ClO_4^- (as its TBA salts); Emission spectra taken upon titration of (b) *cis*-**3** and (d) *trans*-**3** (20 μM, λex = 414 nm) in CH_3CN with CN^-, Inset: Plot of relative emission intensity versus TBACN concentration.

16. The fluorescence detection limit of *tran*-3 and *cis*-3 with CN^- in CH_3CN.

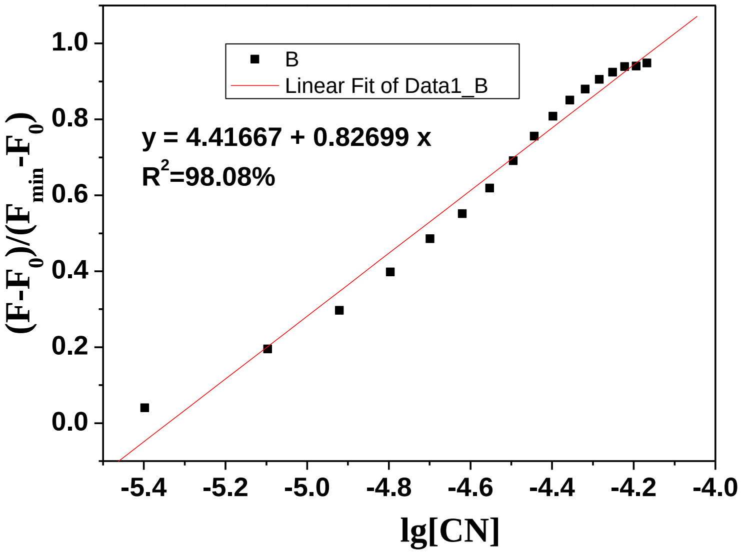

Figure S31. Emission intensity ratio (F_{504}) of *cis*-**3** (20 μM) as a function of CN^- concentration from 0–68 μM (0–3.40 equiv).

Linear Regression for Book1_B:

Equation	Y = A + B * X	
Parameter	Value	Error
A	4.41667	0.13164
B	0.82699	0.0289
R	SD	N
0.99096	0.03996	17

The result of the analysis as follows:

Linear Equation: Y = 4.41667+0.82699* X, R = 0.99096

S= 82.699 * 10^4, K = 3, δ = 0.03996

LOD = K *δ / S = 0.145 μM

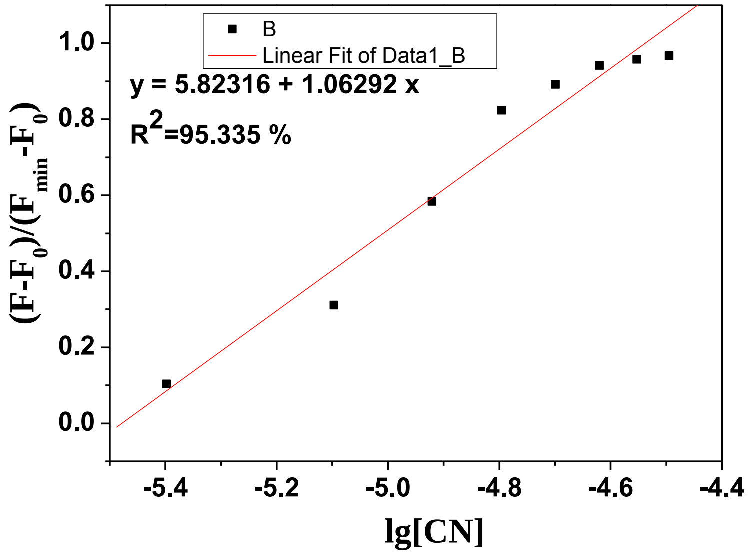

Figure S32. Emission intensity ratio (F_{515}) of *trans*-**3** (20 μM) as a function of CN^- concentration from 0-32 μM (0–1.6 equiv).

Linear Regression for Book1_B:

Equation	Y = A + B * X	
Parameter	Value	Error
A	5.82316	0.42778
B	1.06292	0.08855
R	SD	N
0.97981	0.07157	8

The result of the analysis as follows:

Linear Equation: Y = 5.82316+1.06292* X, R = 0.97981

S= 106.292 * 10^4, K = 3, $\delta = 0.07157$

LOD = K *δ / S = 0.202 μM

17. The ^{1}H NMR titration of *trans*-3 with F$^-$ ions.

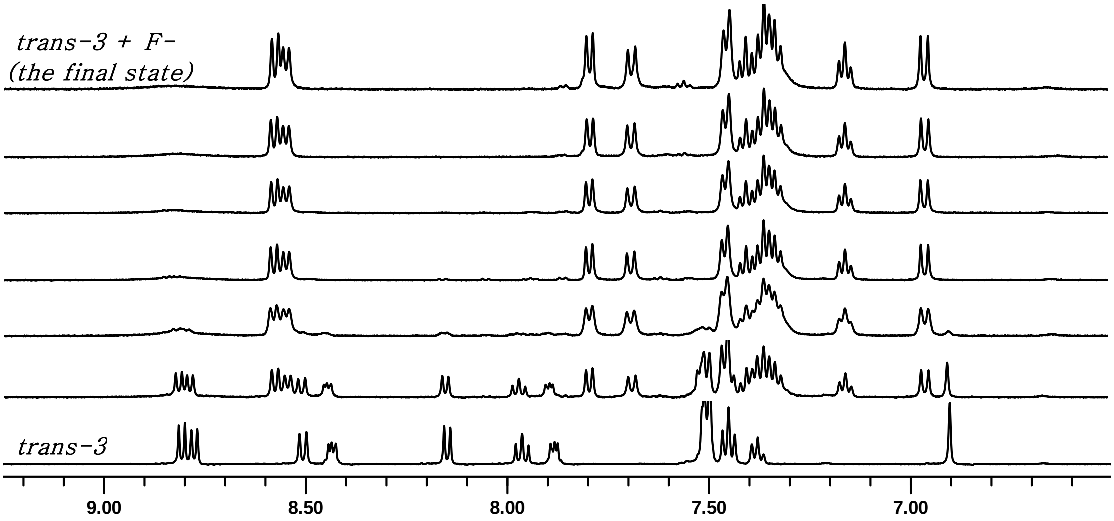

Figure S33. ^{1}H NMR titration spectra of *trans*-**3** in DMSO-d_6 (1.09 × 10^{-2} mol /L) upon addition of F$^-$ ions (as tetrabutylammonium salts in DMSO-d_6) at 298 K, from the bottom to top:0, 0.5, 1.0, 1.5, 2.5, 4.5, 6.5 equiv.

18. The DFT calculations of *trans*-3 with CN⁻ ions.

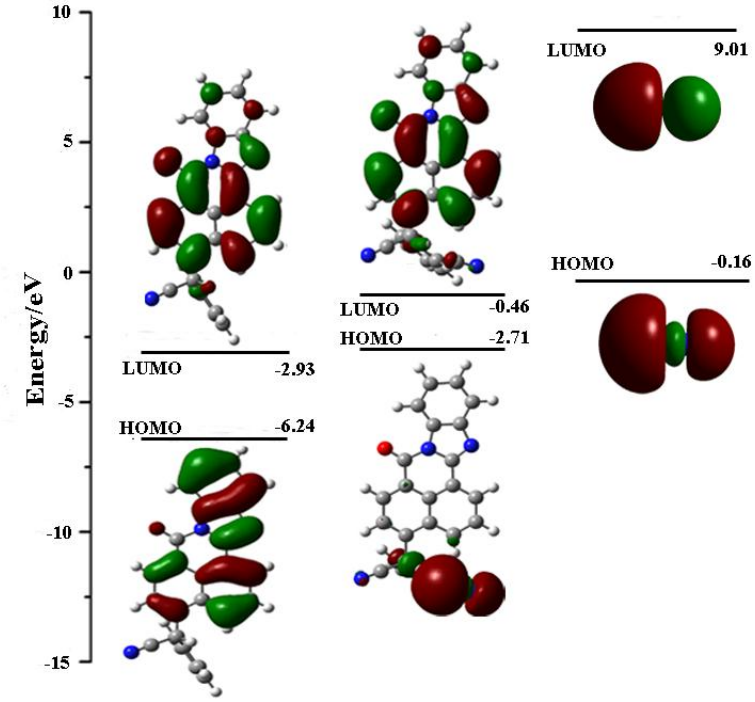

Figure S34. HOMO-LUMO energy levels and the interfacial plots of the orbitals for *trans*-**3** and the *trans*-**3** + CN⁻ complex.